Introduction of Si PERC Rear Contacting Design to Boost Efficiency of Cu(In,Ga)Se_2 Solar Cells

Bart Vermang, Jörn Timo Wätjen, Christopher Frisk, Viktor Fjällström, Fredrik Rostvall, Marika Edoff, Pedro Salomé, Jérôme Borme, Nicoleta Nicoara, and Sascha Sadewasser

***Abstract*—Recently, Cu(In,Ga)Se_2 (CIGS) solar cells have achieved 21% world-record efficiency, partly due to the introduction of a postdeposition potassium treatment to improve the front interface of CIGS absorber layers. However, as high-efficiency CIGS solar cells essentially require long diffusion lengths, the highly recombinative rear of these devices also deserves attention. In this paper, an Al_2O_3 rear surface passivation layer with nanosized local point contacts is studied to reduce recombination at the standard Mo/CIGS rear interface. First, passivation layers with well-controlled grids of nanosized point openings are established by use of electron beam lithography. Next, rear-passivated CIGS solar cells with 240-nm-thick absorber layers are fabricated as study devices. These cells show an increase in open-circuit voltage (+57 mV), short-circuit current (+3.8 mA/cm^2), and fill factor [9.5% (abs.)], compared with corresponding unpassivated reference cells, mainly due to improvements in rear surface passivation and rear internal reflection. Finally, solar cell capacitance simulator (SCAPS) modeling is used to calculate the effect of reduced back contact recombination on high-efficiency solar cells with standard absorber layer thickness. The modeling shows that up to 50-mV increase in open-circuit voltage is anticipated.**

***Index Terms*—Al_2O_3, Cu(In,Ga)Se_2, electron beam lithography, local point contacts, nanosized openings, passivation layer, passivated emitter and rear cell (PERC), rear internal reflection, rear surface recombination velocity, Si.**

I. Introduction

OVER the past two years, CIGS solar cells have taken a sudden leap in world record efficiency of 1%, from around 20% to 21% [1]. Before 2013, CIGS solar cell efficiency improvements were mainly due to enhancements in absorber material quality, and cell efficiencies were lingering around 20% for a few years—as achieved by National Renewable Energy Laboratory (NREL) and the Centre for Solar Energy and Hydrogen Research Baden-Württemberg (ZSW) [2]. However, in 2013, a major breakthrough to reach 20.4% has been achieved by the Swiss Federal Laboratories for Materials Science and Technology (Empa), which rapidly inspired ZSW, Solar Frontier, and Solibro (Hanergy Group) to reach 20.8%, 20.9%, and even 21%, respectively [3]–[5].

This rise in efficiency has been triggered by the introduction of a postdeposition potassium (K) treatment to improve the front interface of CIGS absorber layers. It has been shown that this K treatment results in enhanced passivation (grain boundaries and donor-like defects), thinning of the CdS buffer layer, increased junction depth, and increased bandgap (larger Ga content) (see [3], [4], and [6]). Hence, the postdeposition treatment mainly causes improvements in open-circuit voltage ($V_{\rm OC}$), but also in short-circuit current density ($J_{\rm SC}$—resulting from a higher transparency of the CdS layer). Roughly speaking, it can be said that all these improvements are located in the front part of high-efficiency solar cells (buffer–absorber).

However, as high-efficiency CIGS solar cells essentially have long diffusion lengths, the highly recombinative rear of these devices would be the next region of attention. CIGS absorber layer thicknesses in high-efficiency devices are between 2.5 and 3.0 μm [3], [4], while effective minority carrier diffusion lengths are anticipated to be between 1.5 and 2.0 μm [7]. Thus, absorber layer thicknesses between 1.5 and 2.0 μm should be sufficient from optical perspective, but thicker absorbers are required as recombination is high at standard Mo/CIGS (absorber–rear contact) rear interfaces. This highly recombinative rear interface becomes very obvious as a loss in $V_{\rm OC}$ if the absorber thickness is reduced [8], [9].

One method to reduce recombination at the standard Mo/CIGS rear interface is the introduction of a rear surface passivation layer with nanosized contacts [8]. This idea stems from the Si solar cell industry, where at the rear of advanced cell concepts rear surface passivation layers are combined with micron-sized point openings—e.g., passivated emitter and rear cells (PERC), as named in the title [10]. Such a passivation layer is known to reduce interface recombination by chemical [equals a reduction in interface trap density ($D_{\rm it}$)] and field-effect passivation (equals a fixed charge density (Q_f) in the passivation layer that reduces the surface minority or majority charge carrier concentration), while the point openings allow for contacting [11].

Previously, two industrially viable rear surface passivation approaches have been developed as proof-of-principles, resulting in rear-surface-passsivated CIGS solar cells with suboptimized grids of local rear contacts. In both processes, Al_2O_3 is used as CIGS surface passivation layer because of similar arguments

Manuscript received July 1, 2014; revised August 15, 2014; accepted August 18, 2014. Date of publication September 4, 2014; date of current version October 17, 2014. This work was supported by the European Commission via FP7 Marie Curie IEF 2011 Action No. 300998 and FP7 Marie Curie IEF 2012 Action No. 327367, respectively, and in part by the Swedish Science Foundation (VR) and the Swedish Energy Agency.

B. Vermang, J. T. Wätjen, C. Frisk, V. Fjällström, F. Rostvall, and M. Edoff are with the Ångström Solar Center, Division of Solid State Electronics, Department of Engineering Sciences, Uppsala University, 75121 Uppsala, Sweden (e-mail: Bart.Vermang@angstrom.uu.se; timo.watjen@angstrom.uu.se; christopher.frisk@angstrom.uu.se; viktor.fjallstrom@angstrom.uu.se; fredrik.rostvall@angstrom.uu.se; marika.edoff@angstrom.uu.se).

P. Salomé, J. Borme, N. Nicoara, and S. Sadewasser are with the International Iberian Nanotechnology Laboratory, 4715-330 Braga, Portugal (e-mail: pedrosalome@gmail.com; jerome.borme@inl.int; nicoleta.nicoara@inl.int; sascha.sadewasser@inl.int).

Color versions of one or more of the figures in this paper are available online at http://ieeexplore.ieee.org.

Digital Object Identifier 10.1109/JPHOTOV.2014.2350696

made as for its use as Si surface passivation layer [8], [11]. The processes differ in contacting 1) local point contacts are used, as generated by the formation of nanosphere-shaped precipitates in chemical bath deposition (CBD) of CdS [8], [9], [12], or 2) Mo nanoparticles as contacts are used, as grown in a highly ionized pulsed plasma [13], [14]. Both approaches have been integrated in CIGS solar cells with ultrathin ($\leq$500 nm, [15], [16]) absorber layers showing an increase in $V_{\rm OC}$ and $J_{\rm SC}$ compared with corresponding unpassivated reference cells, which can be explained by an improvement in rear surface passivation and optical confinement, respectively. However, in both cases, the point contacting grids are only suboptimized as can be seen from an increase in series resistance (R_s) compared with the unpassivated reference cells.

In this paper, rear-surface-passivated CIGS solar cells with well-controlled grids of nanosized local rear point contacts are established and studied. First, an e-beam lithography process has been developed to generate well-controlled grids of nanosized point openings in Al_2O_3 passivation layers. Next, this point-opened Al_2O_3 rear surface passivation layer is integrated in ultrathin CIGS solar cells to assess its surface passivation, rear internal reflection (R_b), and contacting properties. Finally, the potential of this advanced rear contacting structure in high-efficiency CIGS solar cells with thick absorber layers is modeled.

II. Experimental Results

The focus of this experimental section is on the formation of well-controlled grids of nanosized point openings in Al_2O_3 passivation layers by use of electron beam lithography. Before the patterning process, a 420-nm-thick Polymethyl Methacrylate (PMMA) resist is deposited on soda lime glass (SLG)/Mo/Al_2O_3 substrates. First, this resist is exposed in a Vistec EBPG 5200 e-beam lithography system at 100 kV. Each point contact is exposed as a single dot resulting about 460 nm $\times$ 220 nm. An array of 40 $\times$ 20 mm^2 of such dots with reproducible dot shape and 2-μm spacing could be produced in 5.5 h. Then, this resist is developed at room temperature by spray of pure methylisobutylketone (MIBK) for 40 s, using isopropanol as a stopper. Opening of the Al_2O_3 layer is done by reactive ion etching (SPTS ICP), where Mo is etched at 60.8 nm/min, Al_2O_3 at 96.4 nm/min, and PMMA at 297.6 nm/min. Finally, the PMMA resist is removed by acetone.

The established rear surface passivation structures are integrated into SLG/Mo/Al_2O_3/CIGS/CdS/i-ZnO/ZnO:Al/MgF_2 solar cell devices with ultrathin (240 nm) CIGS absorber layers ([Cu]/([Ga] + [In]) = 0.80 to 0.85 and ungraded [Ga]/([Ga] + [In]) = 0.30). These ungraded CIGS absorbers with uniform low Ga distribution are favored to assess rear surface passivation, because of 1) their high reproducibility, 2) their characteristic high-minority carrier diffusion length, and 3) to exclude complementary rear surface passivation effects (e.g., Ga-grading); a detailed description of the applied cell processing steps can be found in [8], [9], [12], and [13] and a summary is given in Table I. Note that compared with [8], [9], [12], and [13], minor changes have been made to the substrate heating arrangement of the coevaporation system.

TABLE I
Overview of All Steps Required to Fabricate Al_2O_3 Rear-Surface-Passivated CIGS Solar Cells With Well-Controlled Grids of Nanosized Local Point Contacts

Step	Description
1	Glass cleaning
2	Mo rear contact sputtering
3	**Al_2O_3 passivation layer deposition**
4	**Creation of openings in this layer by e-beam litho**
5	NaF evaporation
6	Ultra-thin (240 nm) CIGS absorber co-evaporation
7	CBD CdS buffer deposition
8	(i-)ZnO(:Al) window sputtering
9	Ni/Al/Ni front contact evaporation
10	0.5 cm^2 solar cell scribing
11	MgF_2 anti reflection coating

The unpassivated reference cells have the same processing sequence, but without steps 3 and 4.

Light *J–V* and external quantum efficiency (EQE) measurements, scanning electron microscopy with energy dispersive X-ray spectroscopy analysis (SEM-EDX), and the solar cell capacitance simulator (SCAPS 3.2) modeling are performed as described elsewhere [7], [12], [17], [18].

III. Results and Discussion

A. Development of Point-Opened Al_2O_3 Passivation Layers

The applied e-beam lithography process successfully generates well-ordered grids of elliptically shaped nanosized point openings in the Al_2O_3 passivation layers. Fig. 1 displays various pictures of an SLG/Mo/Al_2O_3 (10 nm) sample after the e-beam lithography process: a large-scale optical microscopy image [top view, Fig. 1(a)] shows the long-range regular geometry of the pattern with a narrow dispersion of sizes, and a tapping mode atomic force microscopy (AFM) image [see Fig. 1(b)] shows the elliptical shape of the openings and the regular 2-μm spacing. The corresponding height profile obtained along the indicated line in Fig. 1(b) is depicted in Fig. 1(c); from equivalent analysis of several samples, the depth of these holes is determined to be 15 $\pm$ 5 nm, thus indicating a slight overetching into the Mo layer. Furthermore, the same sample is analyzed by SEM-EDX and the Mo M, Al K, and O K images are shown in Fig. 1(d). In addition, this picture shows that a grid of well-opened holes is generated in the passivation layer after the e-beam lithography process.

B. Integration Into Ultrathin Cu(In,Ga)Se_2 Solar Cells

Introduction of this well-controlled nanosized point-opened Al_2O_3 rear surface passivation layer in ultrathin CIGS solar cells leads to an increase in $V_{\rm OC}$, $J_{\rm SC}$, and even fill factor (FF), thanks to an improvement in rear surface passivation and rear internal reflection. Table II gives an overview of average cell characterization results of unpassivated reference CIGS solar cells and Al_2O_3 rear-surface-passivated cells with well-controlled grids

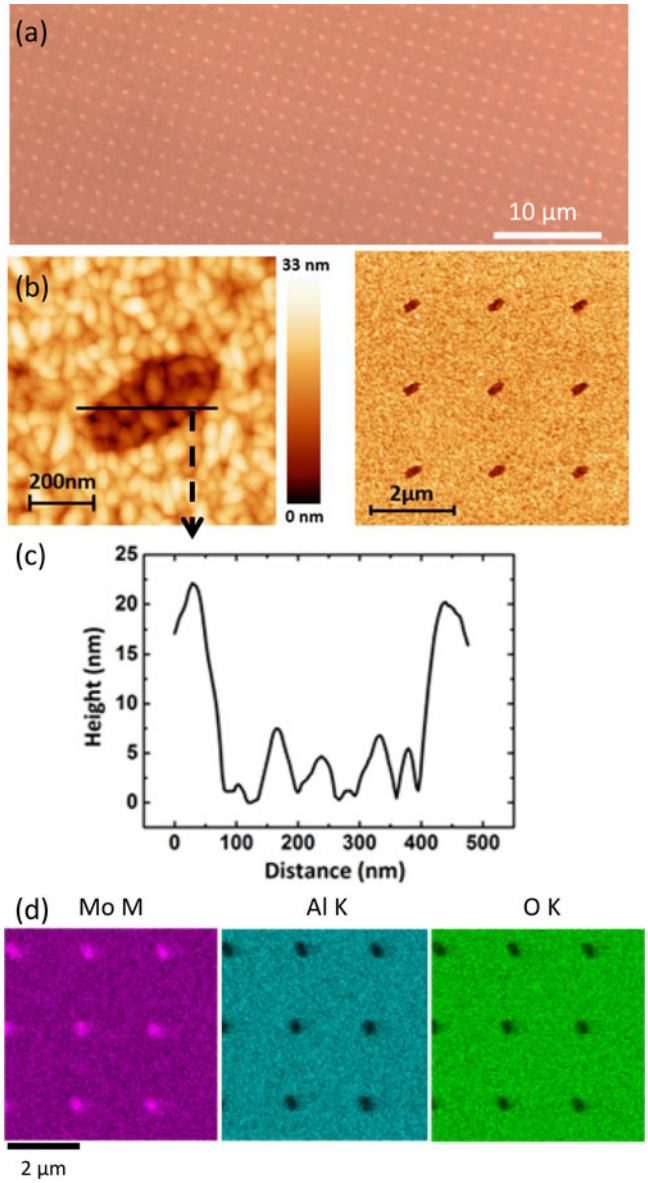

Fig. 1. SLG/Mo/Al_2O_3 (10 nm) sample after the e-beam lithography process. (a) (Top-view) Optical microscopy image, (b) tapping mode atomic force microscopy topography image, (c) corresponding height profile obtained along the indicated line, and (d) scanning electron microscopy with energy dispersive X-ray spectroscopy analysis images for Mo, Al, and O.

TABLE II
AVERAGE CELL CHARACTERIZATION RESULTS (AM1.5 G) FOR 0.5 cm^2 UNPASSIVATED REFERENCE CIGS SOLAR CELLS AND Al_2O_3 REAR-SURFACE-PASSIVATED CELLS WITH WELL-CONTROLLED GRIDS OF NANOSIZED LOCAL REAR POINT CONTACTS

Description	# cells	V_{OC} (mV)	J_{SC} (mA/cm^2)	FF (%)	Eff. (%)
Unpass. ref.	4	602 ±6	19.6 ±0.1	67.6 ±2.9	8.0 ±0.3
Al_2O_3 rear pass.	4	659 ±5	23.3 ±0.5	77.0 ±0.6	11.8 ±0.3

GGI is depth-uniform and equals 30%.
The CIGS absorber layer thickness is 240 nm.

of nanosized local rear point contacts; both cell types have the same absorber layer thickness of 240 nm only. A cross-sectional

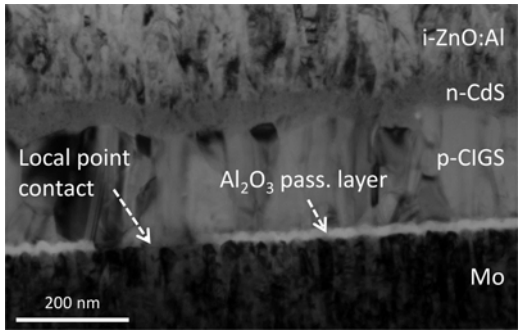

Fig. 2. Transmission electron microscopy cross-section image of an Al_2O_3 rear-surface-passivated cell with a well-controlled grid of nanosized local rear point contacts.

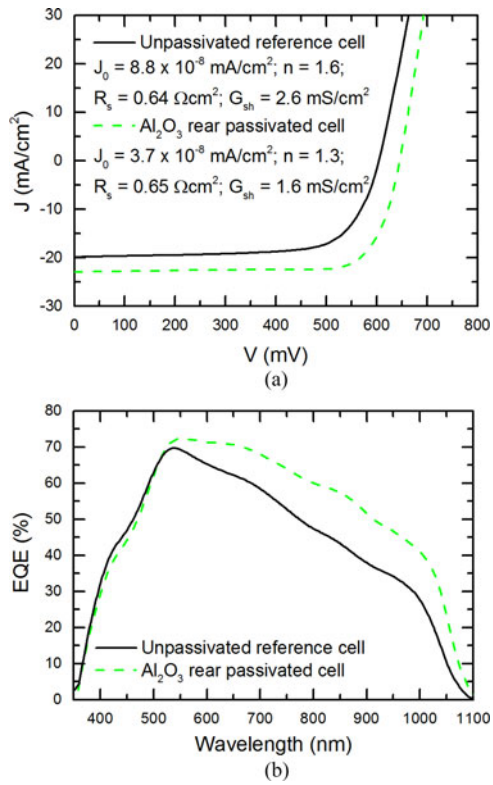

Fig. 3. Representative (a) *J–V* and (b) external quantum efficiency curves for Al_2O_3 rear-surface-passivated CIGS solar cells with well-controlled grids of nanosized local rear point contacts and corresponding unpassivated reference cells. GGI is depth-uniform and equals 30%; the CIGS absorber layer thickness is 240 nm. In (a), the dark saturation current density, ideality factor, series resistance, and shunt conductance are presented, as estimated from the one-diode model [19].

TEM picture of such an Al_2O_3-rear-passivated cell is shown in Fig. 2, which clearly displays the Al_2O_3 passivation layer (25–30 nm) and a local point contact (also showing an unchanged Mo layer after etching). Additionally, Fig. 3 shows representative *J–V* and EQE curves for the rear-passivated cells and corresponding unpassivated reference cells of Table II. In Fig. 3(a), also the dark saturation current density (J_0), ideality factor (n), R_s, and shunt conductance (G_{sh}) are given, as estimated from the one-diode model [19]. Comparing the rear-passivated cell

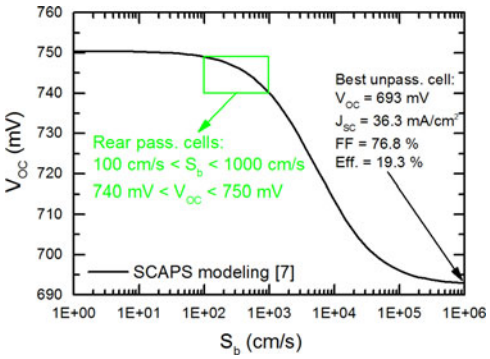

Fig. 4. Simulated open-circuit voltage as a function of surface recombination velocity applying a SCAPS model of high-efficiency CIGS solar cells made at the Ångström Solar Center (without KF post-deposition treatment). This SCAPS model has been described in [7].

results with the corresponding reference cell results, there is 1) a clear increase in $V_{\rm OC}$ (+57 mV), mainly due to significant improvement in rear surface passivation as indicated by a clear decrease in J_0 (see also [8] for a discussion based on SCAPS modeling); 2) a clear increase in $J_{\rm SC}$ (+3.8 mA/cm^2), mainly due to significant improvement in rear internal reflection as indicated by a clear increase in EQE for all wavelengths >550 nm [see Fig. 3(b)]; see also [8], [9], and [12] for detailed R_b calculations); and 3) a clear increase in FF (+9.5% (abs.)), as the R_s is the same for both cells while the rear-passivated cells show an increased $V_{\rm OC}$ and decreased n and $G_{\rm sh}$. Hence, the average efficiency of the rear-passivated cells is 3.9% (abs.) higher than the efficiency of the corresponding unpassivated reference cells. Note that initial results indicate that the larger $G_{\rm sh}$ for unpassivated thin CIGS solar cells is caused by light-dependent shunt-like behavior, but a discussion is left out of this paper as its investigation is still ongoing.

C. Modeling of Thick Cu(In,Ga)Se_2 Solar Cells

SCAPS simulations indicate that the rear surface passivation approach also has potential to considerably increase $V_{\rm OC}$ of high-efficiency CIGS solar cells (with standard absorber layer thickness), due to their inherent long diffusion lengths. The best CIGS solar cell (without KF posttreatment) made at the Ångström Solar Center, has $V_{\rm OC}$ 693 mV, $J_{\rm SC}$ 36.3 mA/cm^2, FF 76.8%, and thus an efficiency of 19.3%, as independently confirmed by FhG-ISE CalLab. These cells have been extensively modeled using SCAPS [7], and in Fig. 4 this model is used to see the effect of decreased rear surface recombination velocity (S_b) on $V_{\rm OC}$. The figure indicates that up to 50 mV increase in $V_{\rm OC}$ can be expected if S_b is between 100 and 1000 cm/s. This large $V_{\rm OC}$ enhancement for rear-passivated high-efficiency CIGS solar cells is to be expected since these cells should—according to the modeling—have long diffusion lengths. Therefore, reducing recombination at the rear will have a substantial impact. Note that 1) for the presented rear surface passivation approach S_b below 1000 cm/s is considered to be viable, as already discussed in [8], and 2) the CIGS thickness has not been fine tuned in this modeling, which could increase $V_{\rm OC}$ even further.

IV. Conclusion and Outlook

In summary, Al_2O_3 rear-surface-passivated CIGS solar cells with well-controlled grids of nanosized local rear point contacts are developed using e-beam lithography technology. Using thin CIGS absorber layers, these cells show a clear increase in all cell characteristics compared with corresponding unpassivated reference cells. The most important advances are a clear increase in $V_{\rm OC}$ due to improved rear surface passivation, a clear increase in $J_{\rm SC}$ due to enhanced rear internal reflection, and a clear increase in FF due to the higher $V_{\rm OC}$ and more ideal cell behavior. Additionally, SCAPS has been used to model the impact of this rear surface passivation approach on high-efficiency solar cells with standard absorber layer thickness. Also in this case, the modeling results indicate a significant increase in $V_{\rm OC}$ for the rear-passivated high-efficiency CIGS solar cells, due to their inherent long diffusion lengths.

In the future, this established rear surface passivation approach will be used to 1) optimize the size of and distance between the local point openings and 2) fabricate solar cell devices to study current transport in the absorber layers. Additionally, 3) integration of the rear surface passivation structure in tangible high-efficiency solar cells is ongoing.

References

[1] M. A. Green, K. Emery, Y. Hishikawa, W. Warta, and E. D. Dunlop, "Solar cell efficiency tables (version 44)," *Prog. Photovoltaics: Res. Appl.*, vol. 22, pp. 701–710, 2014.

[2] (2014, Jun. 26). NREL research cell efficiency records.[Online]. Available: http://www.nrel.gov/ncpv/images/efficiency_chart.jpg

[3] A. Chirilă, P. Reinhard, F. Pianezzi, P. Bloesch, A. R. Uhl, C. Fella, L. Kranz, D. Keller, C. Gretener, H. Hagendorfer, D. Jaeger, R. Erni, S. Nishiwaki, S. Buecheler, and A. N. Tiwari, "Potassium-induced surface modification of Cu(In,Ga)Se_2 thin films for high-efficiency solar cells," *Nature Mater.*, vol. 12, pp. 1107–1111, 2013.

[4] P. Jackson, D. Hariskos, R. Wuerz, W. Wischmann, and M. Powalla, "Compositional investigation of potassium doped Cu(In,Ga)Se_2 solar cells with efficiencies up to 20.8%," *Phys. Status Solidi RRL*, vol. 8, no. 3, pp. 219–222, 2014.

[5] Solibro GmbH, "CIGS module manufacturing with high deposition rates and efficiencies," presented at the 40th IEEE Photovoltaic Spec. Conf., Denver, CO, USA, Jun. 11, 2014.

[6] A. Laemmle, R. Wuerz, and M. Powalla, "Efficiency enhancement of Cu(In,Ga)Se_2 thin-film solar cells by a post-deposition treatment with potassium fluoride," *Phys. Status Solidi RRL*, vol. 7, no. 9, pp. 631–634, 2013.

[7] C. Frisk, C. Platzer-Björkman, J. Olsson, P. Szaniawski, J. T. Wätjen, V. Fjällström, P. Salomé, and M. Edoff, "Modeling Ga-profiles for Cu(In,Ga)Se_2 thin film solar cells with varying defect density," in *Proc. 23rd Int. Photovoltaic Sci. Eng. Conf.*, 2013, pp. 1192–2013.

[8] B. Vermang, V. Fjällström, J. Pettersson, P. Salomé, and M. Edoff, "Development of rear surface passivated Cu(In,Ga)Se_2 thin film solar cells with nano-sized local rear point contacts," *Sol. Energy Mater. Sol. Cells*, vol. 117, pp. 505–511, 2013.

[9] B. Vermang, V. Fjällström, X. Gao, and M. Edoff, "Improved rear surface passivation of Cu(In,Ga)Se_2 solar cells: A combination of an Al_2O_3 rear surface passivation layer and nanosized local rear point contacts," *IEEE J. Photovoltaics*, vol. 4, no. 1, pp. 486–492, 2014.

[10] J. Zhao, A. Wang, and M. A. Green, "24% efficient PERL structure silicon solar cells," in *Proc. 21st IEEE Photovoltaic Spec. Conf.*, 1990, pp. 333–335.

[11] G. Dingemans and W. M. M. Kessels, "Review: Status and prospects of Al_2O_3-based surface passivation schemes for silicon solar cells," *J. Vac. Sci. Technol. A*, vol. 30, no. 4, pp. 040802-1–040802-27, 2012.

[12] B. Vermang, J. T. Wätjen, V. Fjällström, F. Rostvall, M. Edoff, R. Kotipalli, F. Henry, and D. Flandre, "Employing Si solar cell technology to increase efficiency of ultra-thin Cu(In,Ga)Se_2 solar

cells," *Prog. Photovoltaics: Res. Appl.*, DOI: 10.1002/pip.2527, see http://onlinelibrary.wiley.com/doi/10.1002/pip.2527/abstract
[13] B. Vermang, J. T. Wätjen, V. Fjällström, F. Rostvall, M. Edoff, R. Gunnarsson, I. Pilch, U. Helmersson, R. Kotipalli, F. Henry, and D. Flandre, "Highly reflective rear surface passivation design for ultra-thin Cu(In,Ga)Se_2 solar cells," *Thin Solid Films*, to be published.
[14] I. Pilch, D. Söderström, N. Brenning, and U. Helmersson, "Size-controlled growth of nanoparticles in a highly ionized pulsed plasma," *Appl. Phys. Lett.*, vol. 102, pp. 033108-1–033108-4, 2013.
[15] W. N. Shafarman, R. S. Huang, and S. H. Stephens, "Characterization of Cu(InGa)Se_2 solar cells using etched absorber layers," in *Proc. IEEE 4th World Conf. Photovoltaic Energy Convers.*, 2006, pp. 420–423.
[16] J. K. Larsen, H. Simchi, P. Xin, K. Kim, and W. N. Shafarman, "Backwall superstrate configuration for ultrathin Cu(In,Ga)Se_2 solar cells," *Appl. Phys. Lett.*, vol. 104, pp. 033901-1–033901-4, 2014.
[17] J. T. Wätjen, *Microscopic Characterisation of Solar Cells*. Uppsala, Sweden: Univ. of Uppsala, 2013.
[18] M. Burgelman, P. Nollet, and S. Degrave, "Modelling polycrystalline semiconductor solar cells," *Thin Solid Films*, vol. 361–362, pp. 527–532, 2000.
[19] U. Malm, *Modelling and Degradation Characteristics of Thin-Film CIGS Solar Cells.* Uppsala, Sweden: Univ. of Uppsala, 2008.

Bart Vermang received the M.Sc. degree in experimental physics from the University of Ghent, Ghent, Belgium, and the Ph.D. degree in electrical engineering from the University of Leuven, Leuven, Belgium, in 2005 and 2012, respectively.

During his M.Sc. final research project, he studied surface reactions in model metallic catalyst systems with the Norwegian University of Science and Technology, Trondheim, Norway. He performed his Ph.D. research with Imec in Belgium, where he developed novel surface passivation structures for industrial silicon solar cells. He is currently a Postdoctoral Researcher with the University of Uppsala, Uppsala, Sweden, where his challenge is to integrate progressive Si solar cell concepts in CIGS thin-film cells.

Jörn Timo Wätjen received the Diploma degree in physics from RWTH Aachen, Aachen, Germany, in 2008 and the Ph.D. degree in solid-state electronics from Uppsala University, Uppsala, Sweden, in 2013.

He conducted his diploma research project with the Forschungszentrum Jülich, Germany, studying the influence of back reflectors in thin-film silicon solar cells. During his Ph.D. work, he studied the growth of CIGS and focused on electron microscopy-based techniques for characterization of CIGS and CZTS solar cells. His current research interests include CIGS and CZTS solar cells with Uppsala University.

Christopher Frisk received the M.Sc. degree in physics from the University of Gothenburg, Göteborg, Sweden, in Spring 2012. The topic of his Master thesis was photoelectrochemical solar cells using synthesized CdS quantum dots. In fall 2012, he started the Ph.D. degree at Ångström Solar Center, (A°SC) Uppsala, where his main focus was on device simulations and related electrical and optical characterization.

He is currently working with both CIGS and CZTS at ÅSC.

Viktor Fjällström was born in Uddevalla, Sweden, in 1986. He received the Master's degree in energy systems engineering from Uppsala University, Uppsala, Sweden, in 2010.

The main focus of his studies was renewable energy. His Master thesis was based on experiments in the field of concentrated solar power. Since the end of 2010, he has been a Research Engineer with the Thin Film Solar Cell Group, Division of Solid State Electronics, Uppsala University.

Fredrik Rostvall received the Master's thesis in material science from the Thin Film Solar Cell Group, Uppsala University, Uppsala, Sweden, in 2014.

His main focus was on improving the lifetime of CIGS solar cells. He is currently continuing his work at the university.

Marika Edoff received the M.Sc. degree in electrical engineering and the Ph.D. degree in solid-state electronics from the Royal Institute of Technology, Stockholm, Sweden, in 1990 and 1997, respectively.

Since 2003, she has been leading research activities on solid-state thin-film solar cells with Uppsala University, Uppsala, Sweden. She was one of the four founders of Solibro, where since 2005, she has also been a part-time employee. Her research interests include CIGS-based thin-film solar cells with a focus on material synthesis and device characterization.

Pedro Salomé received the Diploma degree in physics engineering and the Ph.D. degree in physics from the University of Aveiro, Aveiro, Portugal, in 2006 and 2011, respectively.

During his Ph.D. studies, he was involved in research on growth and characterization of Cu(In,Ga)Se_2 and $Cu_2ZnSn(S,Se)_4$ thin films for solar cell applications. From 2011 to early 2013, he was with Uppsala University, Uppsala, Sweden, where he studied the impact of substrate properties on the performance of Cu(In,Ga)Se_2 thin film solar cells in a collaboration with Corning Inc. In 2013, he moved to the International Iberian Nanotechnology Laboratory with a Marie Curie Intra European Fellowship to work with nanostructures for high-efficiency solar cells. His research interests include CIGS solar cells and characterization of semiconductors.

Jérôme Borme received the engineering degree from École Centrale de Lyon, Écully, France, in 2002 and the Ph.D. degree in physics from Université Joseph Fourier, Grenoble, France, in 2006.

As a Postdoctoral Researcher, he worked on the design, fabrication, and use of magneto-resistive micro and nanosensors for mechanical positioning (2006–2010). He studied the properties of graphene nanoislands by scanning microscopies as a Visitor at Max-Planck-Institut für Mikrostrukturphysik, Halle (Saale), Germany (2010–2011). Since May 2011, he has been with the International Iberian Nanotechnology Laboratory as a Postdoctoral Researcher with research interests in graphene nanodevices and, since July 2012, he has been as a Staff Researcher responsible for nanolithography processes.

Nicoleta Nicoara received the Diploma degree in physics from the Babes-Bolyai University, Cluj-Napoca, Romania, and the Ph.D. degree in condensed matter physics from Universidad Autónoma de Madrid, Madrid, Spain, in 2007.

Her work was focused on the structural and electronic characterization of organic/inorganic semiconductor interfaces. As a Postdoctoral Researcher, she was with the Universidad Autónoma de Madrid (2007–2011), where she was involved in the development, design, and construction of a low-temperature scanning probe microscope for atomic scale characterization of low-dimensional systems. Since May 2011, she has been a Research Fellow with the International Iberian Nanotechnology Laboratory, Braga, Portugal, focusing on the characterization of chalcopyrite-type quantum dots for solar cells by scanning probe microscopies.

Sacha Sadewasser received the Diploma degree in physics from the RWTH Aachen, Aachen, Germany, and the Ph.D. degree from the Washington University, St. Louis, MO, USA, in 1999.

From 1999–2011, he was with the Helmholtz-Zentrum Berlin (HZB; the former Hahn-Meitner Institute), interrupted by a Ramón y Cajal fellowship with the Centro Nacional de Microelectónica, Barcelona, Spain, from 2003 to 2004. He was the Deputy Head of the Department for Heterogeneous Material systems at HZB from 2008–2011, before taking a Group Leader position of the Laboratory for Nanostructured Solar Cells with the International Iberian Nanotechnology Laboratory, Braga, Portugal.